

Precise extrapolation of the correlation function asymptotics in uniform tensor network states with application to the Bose-Hubbard and XXZ models

Marek M. Rams,¹ Piotr Czarnik,² and Lukasz Cincio³

¹*Institute of Physics, Jagiellonian University, Łojasiewicza 11, PL-30348 Kraków, Poland*

²*Institute of Nuclear Physics, Polish Academy of Sciences, Radzikowskiego 152, PL-31342 Kraków, Poland*

³*Theory Division, Los Alamos National Laboratory, Los Alamos, NM 87545, USA*

We analyze the problem of extracting the correlation length from infinite matrix product states (MPS) and corner transfer matrix (CTM) simulations. When the correlation length is calculated directly from the transfer matrix, it is typically significantly underestimated for finite bond dimensions used in numerical simulation. This is true even when one considers ground states at a distance from the critical point. In this article we introduce extrapolation procedure to overcome this problem. To that end we quantify how much the dominant part of the MPS/CTM transfer matrix spectrum deviates from being continuous. The latter is necessary to capture the exact asymptotics of the correlation function where the exponential decay is typically modified by an additional algebraic term. By extrapolating such a refinement parameter to zero, we show that we are able to recover the exact value of the correlation length with high accuracy. In a generic setting, our method reduces the error by a factor of ~ 100 as compared to the results obtained without extrapolation and a factor of ~ 10 as compared to simple extrapolation schemes employing bond dimension. We test our approach in a number of solvable models both in 1d and 2d. Subsequently, we apply it to one-dimensional XXZ spin- $\frac{3}{2}$ and the Bose-Hubbard models in a massive regime in the vicinity of Berezinskii–Kosterlitz–Thouless critical point. We then fit the scaling form of the correlation length and extract the position of the critical point and obtain results comparable or better than those of other state-of-the-art numerical methods. Finally, we show how the algebraic part of the correlation function asymptotics can be directly recovered from the scaling of the dominant form factor within our approach.

I. INTRODUCTION

Tensor networks and related numerical renormalization group techniques allow to efficiently approximate systems of exponentially many degrees of freedom with manageable number of a few relevant ones, providing invaluable tools in the studies of strongly correlated systems. We are particularly interested in one such technique, based on the matrix product state (MPS) representation of a many-body wave function¹. It provides underlying framework behind a family of state-of-the-art methods for approximating the low energy states of local one-dimensional Hamiltonians^{2–4}, descendant of seminal density matrix renormalization group (DMRG) algorithm^{5,6}. Closely related, corner transfer matrix (CTM) algorithm^{7,8} is used to numerically solve classical systems in 2d, and is a method of choice for contracting 2d quantum states described by projected entangled pair states (PEPS) ansatz^{9,10}.

In this article we address the problem of precise extrapolation of the correlation length in such simulations. Correlation length is a fundamental quantity in the description of (quantum) many-body systems and their phase transitions. It provides valuable input into the nature of the phase being described, as well as informs about its boundaries. Apart from this general consideration, there are two immediate applications of presented method that we mention below. Firstly, it allows to fit the scaling form of the correlation length in the vicinity of the Berezinskii–Kosterlitz–Thouless critical point in one dimensional Bose-Hubbard and XXZ type models.

Besides precisely extracting the critical point position, the accurate knowledge of the scaling form is relevant, for instance, to understand the behaviour of quantum fidelity in such systems¹¹. Secondly, it is desirable to establish reliable method to calculate the correlation length of PEPS using CTM algorithm. This can be applied to characterize the critical behavior of 2d quantum systems at finite temperature within the PEPS approach¹².

Below we focus the discussion on MPS and notice that the argument could also be directly applied to CTM. It is well known that MPS with finite bond dimension is able to reproduce the ground state of local gapped Hamiltonian up to an error which vanishes exponentially with the bond dimension¹³. Consequently, local observables can usually be simulated with similar precision. The correlation length, on the other hand, describes the tail of the correlation function. This tail is vanishing exponentially and as such there is no reason to expect that MPS would be able to capture it faithfully. More importantly, asymptotics of the correlation function calculated for MPS with finite bond dimension is purely exponential¹

$$C_{oq}(R) \sim e^{-R/\xi_A}, \quad (1)$$

while typically one expects that the exponential decay is modified by an additional algebraic term,

$$C_{oq}(R) \sim R^{-\eta} e^{-R/\xi}, \quad (2)$$

as, e.g., in the Ornstein-Zernike formula for the correlation function in the context of the Ising-type models^{14,15}. For those reasons, it is not straightforward to faithfully

recover the asymptotics of the correlation function directly from MPS simulations with finite bond dimension. To highlight the problem, for the specific point in the XXZ spin- $\frac{1}{2}$ model which we discuss in details later, MPS with bond dimension 4096 recovers the exact ground state energy with an error of the order of 10^{-12} , but at the same time it is still underestimating the correlation length by a factor of two.

In this article we propose an extrapolation scheme to overcome the above problem. For uniform MPS (CTM) which describes translationally invariant system the correlation length is calculated from the ratio of two largest eigenvalues of the site-to-site (column-to-column) transfer matrix. The spectrum of this transfer matrix is necessarily discrete for finite bond dimension used in the numerical simulations. In order to recover the algebraic part of the correlation function asymptotics in Eq. (2), the spectrum would have to be continuous. In our approach, we look at the distance δ between next dominant transfer matrix eigenvalues, e.g. the second and the third one, and employ it as a measure of deviation from the exact solution. $\delta = 0$ in the limit of the exact representation of the ground state. For a given model, we calculate the MPS correlation length as well as the refinement parameter δ for a number of MPSs with increasing bond dimensions and subsequently extrapolate $\delta \rightarrow 0$ in order to recover the actual value of the correlation length. In order to benchmark our approach we analyze a number of models where the correlation length, or some related properties like the position of the critical point and its universality class, are known analytically. Based on this data we argue that the method proposed in this article is more reliable and produces more accurate results than the one that directly uses the bond dimension as a refinement parameter.

Correlation function asymptotics can be derived from the Euclidian path-integral representation of the ground state and the exact quantum transfer matrix (QTM). In Refs. 16–18 it was argued that MPS transfer matrix can be understood as an approximation of QTM obtained as a result of renormalization procedure akin to Wilson’s numerical renormalization group description of the impurity problem¹⁹. In this picture, the physical spin is interpreted as an impurity in – by construction translationally invariant – QTM, and MPS transfer matrix retains only the degrees of freedom (along virtual, imaginary time direction of the system) relevant for the description of correlations of such impurity. In this article we further build on this intuition and observe how the form factors (i.e. matrix elements of operator transfer matrix in suitable base, defined below) are effectively being renormalized. Most importantly, we argue that the exponent η of the algebraic part of the correlation function asymptotics in Eq. (2) is directly related to how the relevant dominant form factor decays as we approach the exact solution, $\delta \rightarrow 0$ ($D \rightarrow \infty$).

We should finally contrast our approach with the finite entanglement scaling scheme where, in the vicinity

of the critical point, finite MPS correlation length (a result of finite MPS bond dimension) is used similarly to the effective finite size of the system in order to postulate a scaling hypothesis. The position of the critical point and critical exponents can then be extracted by proper renormalization and collapse of the data obtained for different bond dimensions^{20–26}. Our method enables obtaining scaling form of the correlation length without assuming the scaling hypothesis and as such can be used to independently corroborate some of the results found with finite entanglement scaling. We remark that obtaining the correlation length outside the critical regimes is beyond standard finite entanglement scaling schemes as it requires knowledge of a non-universal scaling function. Furthermore, our extrapolations can also be applied beyond scaling regime, or more generally, when it might be impossible to postulate a scaling ansatz. In this context, for instance, it should be possible to apply our method to obtain more precise description of nonequilibrium dynamical properties, such as spreading of the correlations in the excited system. The two methods are equivalent exactly at the critical point as we note that our refinement parameter δ is directly proportional to the inverse of the MPS correlation length in this case.

The rest of the article is organized as follows. In Sec. II we introduce relevant notation focusing on MPS and quantify the general arguments from the introduction. In Sec. III we briefly summarize our method discussing, in particular, how different properties of a studied model can be used to further refine the measure of error used for extrapolation. We benchmark our approach in Sec. IV. We study XY and XXZ spin- $\frac{1}{2}$ models, where the exact value of the correlation length is known. Then we focus on XXZ spin- $\frac{3}{2}$ model and conclude with Bose-Hubbard model with unit filling as a non-trivial implementation of our method. In Sec. V we test our approach in the context of 2d models and their PEPS description. We employ corner transfer matrix method to analyze exactly solvable statistical models: classical 2d Ising model and 8-vertex model. In Sec. VI, we discuss how the exponent of the leading algebraic part of the correlation function naturally emerges within our approach and uncover its connection with the form factors. We conclude in Sec. VII. Appendix A illustrates the problems related with fitting the asymptotic directly, where inaccurate results are obtained away from the critical point. Paradoxically, it is possible to obtain much better results for the critical systems within such approach. This approach is indeed widely used in the literature. Finally, in Appendix B we argue that methods that provide good extrapolation of energy per lattice site are not suited to work well for the correlation length.

II. NOTATION

In this article we focus on infinite, translationally invariant systems. Setting up the notation, uniform matrix

product states take the form

$$|\Psi\rangle = \sum_{\mathbf{s}} \left(\prod_{n \in \mathbb{Z}} A^{s_n} \right) |\mathbf{s}\rangle, \quad (3)$$

where $|\mathbf{s}\rangle = |\dots, s_1, s_2, s_3, s_4, \dots\rangle$ and A^{s_n} are $D \times D$ matrices with parameter D usually referred to as MPS bond dimension.

MPS transfer matrix (TM) is defined in a standard way

$$\mathcal{T}_A = \sum_{s=1}^d \bar{A}^s \otimes A^s. \quad (4)$$

It is the key object in the calculation of the static correlation function. In order to calculate the expectation values related to some operator o it is also convenient to define operator transfer matrix

$$\mathcal{T}_A^o = \sum_{s,r=1}^d o_{s,r} \bar{A}^s \otimes A^r. \quad (5)$$

For larger unit cell consisting of L -sites, i.e. if MPS is translationally invariant only when shifted by L lattice sites (i.e. due to spontaneous breaking of translational symmetry), those L sites are combined into one to calculate transfer matrix in Eqs. (4, 5).

In our approach we focus on the eigenvalues of the transfer matrix \mathcal{T}_A ,

$$\lambda_j = e^{-(\epsilon_j + i\phi_j)L}, \quad (6)$$

with $j = 0, 1, \dots, D^2 - 1$ and $|\lambda_0| > |\lambda_1| \geq |\lambda_2| \geq \dots$. Eq. (6) singles out (minus log of) the absolute value and

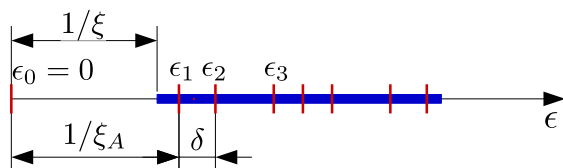


FIG. 1. (Color online) Illustration of the idea behind the scheme. The figure represents (the logarithm of) the dominant part of the transfer matrix spectrum in a generic situation. Blue line represents continuous band necessary to recover the algebraic part of the correlation function asymptotics in Eq. (2). In this case the exact correlation length is set by the gap between the bottom of the band and the origin, $\epsilon_0 = 0$. The spectrum of the transfer matrix for finite bond dimension MPS, represented here by red marks, is necessarily discrete and as such can only approximate the continuous band. Consequently $1/\epsilon_1$ is typically underestimating the true value of the correlation length. We employ $\delta = \epsilon_2 - \epsilon_1$ as a natural measure of how well the discrete spectrum is able to approximate the exact continuous one. By computing $\epsilon_1(D)$ and $\delta(D)$ for some number of MPSs with different bond dimensions D , we extract the correlation length by extrapolating $\delta \rightarrow 0$.

phase into $\epsilon_j \geq 0$ and $\phi_j \in (-\pi/L, \pi/L]$, respectively. We have introduced the period L , so that the correlation length is measured in the units of lattice spacing. Note that some information about phase is lost for $L > 1$. Proper normalization of the state $|\Psi\rangle$ entails that $\lambda_0 = 1$. We additionally assume that the largest value is unique. This ensures the state $|\Psi\rangle$ in Eq. (3) is properly defined.

It is well known that the correlation length ξ_A associated with given normalized MPS is set by the second largest transfer matrix eigenvalue as

$$\xi_A = 1/\epsilon_1, \quad (7)$$

and ϕ_1 captures the leading period of oscillations of the correlation function. More precisely, the connected correlation function of operators o and q at distance R can be expressed as

$$C_{oq}(R) = \langle o_0 q_R \rangle - \langle o_0 \rangle \langle q_R \rangle = \sum_{j>0} f_j^{oq} e^{-(\epsilon_j + i\phi_j)R}, \quad (8)$$

where the form factors f_j^{oq} are defined as

$$f_j^{oq} = (\varphi_0 | \mathcal{T}_A^o | \varphi_j) (\varphi_j | \mathcal{T}_A^q | \varphi_0), \quad (9)$$

with right $|\varphi_j\rangle$ and left $\langle \varphi_j|$ eigenvectors of the transfer matrix normalized as $\langle \varphi_i | \varphi_j \rangle = \delta_{ij}$. Eq. (8) leads to purely exponential decay of asymptotics of the correlation function as in Eq. (1), dictated typically by the second largest eigenvalue of \mathcal{T}_A . Or more generally, by the largest eigenvalues ($j > 0$) for which the corresponding form factors f_j^{oq} are non-zero.

The asymptotics of the correlation function, however, typically contains an algebraic factor as in Eq. (2). For the MPS to recover the algebraic part $R^{-\eta}$ of the asymptotics, the spectrum of the transfer matrix would have to be continuous. This is clearly impossible for the finite bond dimension used in numerical simulations. This is a well known fact in the context of the critical points where the decay of the correlation function is purely algebraic and which is used as one of the arguments why simulating such points with MPS is particularly challenging. As argued above, those issues are still present also far away from the critical point in the context of precise extrapolation of the correlation length.

The discrete dominant eigenvalues of the transfer matrix can at best approximate the continuous spectrum related with the exact quantum transfer matrix, as presented pictorially in Fig. 1. As suggested in that picture, it can be expected that the correlation length obtained as $\xi_A = 1/\epsilon_1$ underestimates the exact value as ϵ_1 would be localized inside the band and not on its edge. Consequently, one has to resort to extrapolation in order to recover the true value of the correlation length.

An alternative approach would be to fit the asymptotics in Eq. (2) for the intermediate values of the distance R . However, away from the critical point, this would require being able to fit the correlation function

asymptotics for distances between the physical correlation length and the length scale resulted from the discreteness of MPS transfer matrix. As we illustrate in the Appendix A, such scale separation might not be accessible in the MPS simulations. The above approach becomes viable at the critical point where there is no physical length scale which has to be respected.

III. SUMMARY OF THE APPROACH

In this article we employ consecutive largest TM eigenvalues to quantify the divergence from the continuous spectrum necessary to capture the algebraic part of the asymptotics. In the simplest case we use the distance between third and second eigenvalue, i.e.

$$\delta = \epsilon_2 - \epsilon_1 \quad (10)$$

as a refinement parameter that measures deviation from the exact solution. If needed, the above simple measure can be further refined by taking into account the fact that some form factors may vanish, transfer matrix can be degenerate and that the system might display some symmetries. The above situations are summarized below and discussed in the subsequent sections of the article.

We calculate $\epsilon_1(D)$ and $\delta(D)$ for a few MPSs obtained for different bond dimensions D , where we observe that the dependence is usually smooth and regular. This allows us to extrapolate $\delta \rightarrow 0$ in order to extract the true value of the correlation length with good precision. We compare this approach with the one where $1/D$ is used as a refinement parameter. We observe that ϵ_1 is significantly less regular as a function of D – especially away from the critical point – and the result of the extrapolation is less reliable. The refinement parameter defined in Eq. (10) proves to be a good starting point, being sufficient in many simpler cases. However, one of the advantages of quantifying the distance from the exact solution using intrinsic quantities calculated for given MPS approximation – in contrast to external parameter such as the bond dimension – is that we can easily take into account additional information about the state to further refine it if necessary. This allows to uncover additional information as well as increase the precision.

Firstly, let us focus only on the part of the transfer matrix spectrum relevant for some particular correlation function $C_{oq}(R)$. To that end, we take into account only transfer matrix eigenvalues for which the corresponding form factors f_j^{oq} are non-zero (within numerical precision), or dominant as compared to the other ones. We mark such eigenvalues with title and additional superscript, $\tilde{\epsilon}_k^{oq}$. In such cases, we define the refinement parameter as

$$\delta = \tilde{\epsilon}_2^{oq} - \tilde{\epsilon}_1^{oq}. \quad (11)$$

We apply this definition throughout the article as the most reliable indicator of which TM eigenvalues are relevant and should be taken into account.

Secondly, dominant TM eigenvalues are usually found in groups with well defined complex phases corresponding to periods of oscillation of the correlation function. Nontrivial correspondence between those phases and the minima of the dispersion relation of the Hamiltonian for which given MPS is the ground state is discussed in Ref. 16. In order to define the refinement parameter we can focus only on part of TM spectrum with given complex phase φ ,

$$\delta = \tilde{\epsilon}_2^\varphi - \tilde{\epsilon}_1^\varphi. \quad (12)$$

We discuss it further in Sec. IV A, where we study the incommensurate phase of the XY model.

Thirdly, there are models for which the dominant TM eigenvalues are either degenerate or are effectively becoming degenerate with the increasing bond dimension. In such case it is necessary to define the refinement parameter as

$$\delta = \epsilon_n - \epsilon_1, \quad (13)$$

where the eigenvalues $\epsilon_1, \dots, \epsilon_{n-1}$ are (near) degenerate. We observe that behavior e.g. for the XXZ spin- $\frac{1}{2}$ model in Sec. IV B where 4 dominant eigenvalues are near-degenerate and we use $n = 5$ in the definition above. More generally, even without degeneracy, any definition of the refinement parameter $\delta = \epsilon_n - \epsilon_1$ with $n > 1$ should lead to the same extrapolated value of the correlation length. In practice, however, we observe that using smaller n allows for more precise results.

Finally, if the system has some local symmetry and MPS is implemented in such a way to take it into account then the TM spectrum splits into groups with well defined symmetry charge u . We can define the refinement parameter using only the eigenvalues belonging to one symmetry sector,

$$\delta = \tilde{\epsilon}_2^u - \tilde{\epsilon}_1^u. \quad (14)$$

This is equivalent to selecting particular subset of correlators corresponding to given symmetry sector. We use the above approach for the XXZ and Bose-Hubbard models in Secs. IV A–IV D, which all have $U(1)$ symmetry.

It should be pointed out that the above features are not independent and can be used simultaneously. Ultimately, the reliability of the extrapolation hinges on consistency of the data obtained for different bond dimensions and through application of different refinement features.

Let us now comment on the extrapolation model that we employ. By analyzing a number of exactly solvable systems we observe that very good results are obtained if one extrapolates by fitting the function

$$\epsilon = \epsilon_e + a\delta^b, \quad (15)$$

where $1/\epsilon_e$ is the extrapolated value of the correlation length and where we assume that the error of the inverse of the correlation function, $\epsilon - \epsilon_{\text{exact}}$, is vanishing as a power law with δ . The exponent b is usually slightly

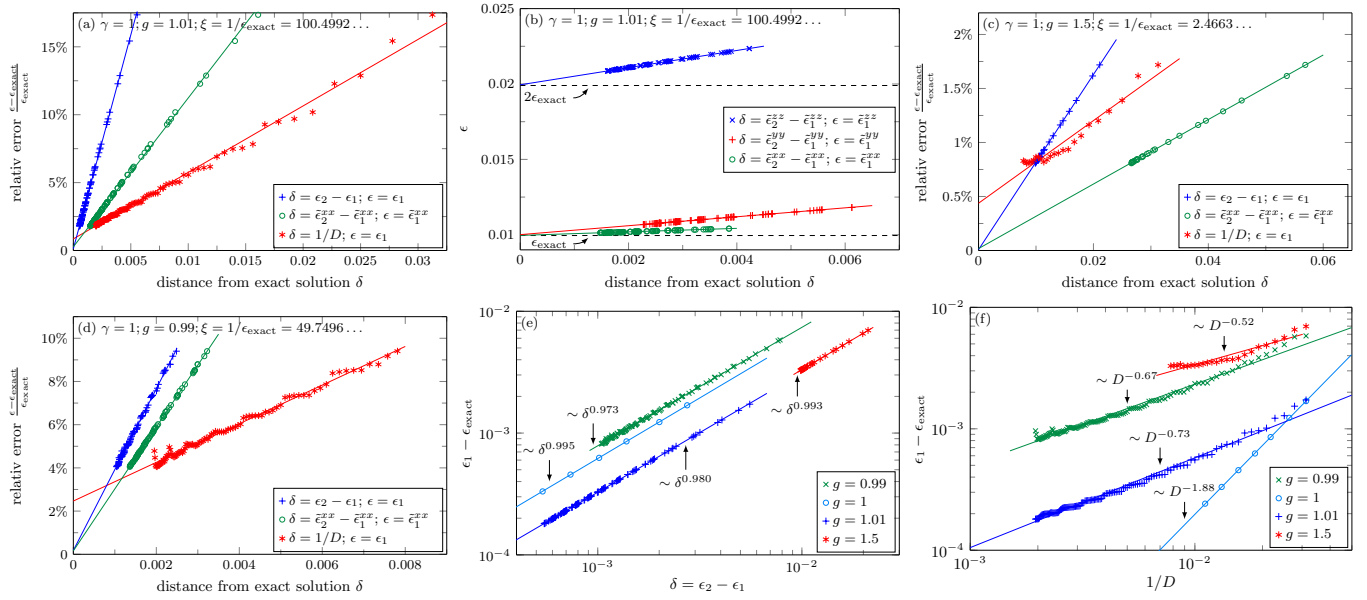


FIG. 2. (Color online) Results for the Ising model, $\gamma = 1$. See text for discussion. Panel (a): paramagnetic phase with $g = 1.01$ and results for bond dimensions $D = 32 \div 512$ with step $dD = 4$. Points represent numerical data and solid lines correspond to linear fits. Panel (b): for $g = 1.01$ each TM eigenvalue (or at least few dominant ones) have nonzero form factor corresponding to exactly one of the correlators $C_{xx}(R)$, $C_{yy}(R)$, $C_{zz}(R)$. This allows to distinguish that the correlation length associated with $C_{zz}(R)$ is halved as compared to the other ones. Here, $D = 128 \div 512$. Panel (c): Results for $g = 1.5$ show that even far away from the critical point $g_c = 1$, extrapolation is necessary to precisely recover the correlation length. Here, $D = 32 \div 128$. Panel (d): results for $g = 0.99$ in the ferromagnetic phase. Panels (e,f): log-log plots show error $\epsilon_1 - \epsilon_{\text{exact}}$ as a function of refinement parameter δ suggested in this article, as well as a function of D . This validates general extrapolation model in Eq. (15) and further shows that extrapolation method based on D is less useful.

smaller than 1 and in many cases linear fit, i.e. fixing $b = 1$ in Eq. (15) proves to be sufficient. It is also a good starting point, which can be then further tested by allowing $b \neq 1$ and checking if this significantly improves the quality of the fit²⁷. We use 95% confidence bounds from the non-linear fit in order to estimate an error of extrapolation. We observe that it provides sensible measure of the quality of the result.

IV. MATRIX PRODUCT STATES SIMULATIONS

In this section we benchmark our approach in a range of models of increasing difficulty. As we move to more difficult models, we illustrate different ways of introducing refinement parameter as briefly discussed in the last section.

A. XY model

We start with the one-dimensional XY model

$$H = - \sum_m \left(\frac{1+\gamma}{2} \sigma_m^x \sigma_{m+1}^x + \frac{1-\gamma}{2} \sigma_m^y \sigma_{m+1}^y + g \sigma_m^z \right), \quad (16)$$

with anisotropy parameter γ and magnetic field g . This model is exactly solvable and the asymptotic form of the connected correlation functions is long known²⁸. We cite the relevant results below. The numerical results in this section were obtained using variational uniform matrix product states algorithm (VUMPS) of Ref. 29, with 1-site unit cell, which is based on the time dependent variational principle approach^{30,31}. All the states for different bond dimensions were converged with norm of the energy gradient below 10^{-12} . Similarly, the maximal change of the Schmidt values in the last iterations of the algorithm (which is another strict measure of convergence) was of the same order.

1. Ising model

We start with the Ising model by setting $\gamma = 1$ in Eq. (16) and note that the TM spectrum is real and positive in this case. We collect the numerical results in Fig. 2 and discuss them below.

In the paramagnetic phase, for $g > 1$, the correlation functions behave asymptotically as $C_{xx}(R) \sim R^{-1/2} e^{-R/\xi}$, $C_{yy}(R) \sim R^{-3/2} e^{-R/\xi}$ and $C_{zz}(R) \sim R^{-2} e^{-2R/\xi}$, where the inverse of the correlation length $1/\xi = \epsilon_{\text{exact}} = \ln g$. Note the additional factor of two in

the exponential part of $C_{zz}(R)$ which is halving the correlation length appearing there. The results for $g = 1.01$ are shown in Fig. 2(a). Several observations are in order. Without extrapolation, even for relatively large bond dimension $D = 512$ for which the smallest Schmidt value of MPS bipartition is of the order of 10^{-14} , the relative error of the correlation length is still $\simeq 2\%$.

The dependence of ϵ_1 on $\delta = \epsilon_2 - \epsilon_1$, Eq. (10), is close to linear. This behavior is seen for the smallest bond dimensions presented on the plot. Linear regression allows for extrapolation of the true correlation length to within relative error $< 0.1\%$, which can be made even smaller by neglecting smallest D shown in the picture. It is interesting to note that the eigenvalues ϵ_1 and ϵ_2 , used here to calculate the distance δ above, contribute to different correlators $C_{xx}(R)$ and $C_{yy}(R)$, respectively. Nevertheless, this approach proves to work well in this model. We obtain consistent result and similar accuracy when we take into account non-zero form factors, and consider only the part of TM spectrum that contributes to $C_{xx}(R)$, i.e. using Eq. (11).

The above can be contrasted with direct application of the bond dimension as a refinement parameter, where the first natural choice is $\delta = 1/D$. In this case ϵ_1 is oscillating as a function of $1/D$, making extrapolation significantly less reliable as it becomes arbitrary which points to choose for extrapolation. Linear regression for $D = 32 \div 512$ recovers correlation length with relative error $\simeq 1\%$, more then an order of magnitude worse then our approach. Indeed, by exploring solvability of the model and in particular its Schmidt spectrum, it was argued in Ref. 17 that ϵ_1 should be approaching the exact value much slower than linearly in $1/D$. This explains why linear regression is still underestimating the true value – a future which for sufficiently large D is shared by all the models studied in this article.

In Fig. 2(b) we focus on parts of TM spectrum contributing to different correlators: $C_{xx}(R)$, $C_{yy}(R)$ and $C_{zz}(R)$. In case of paramagnetic Ising model we observe that each eigenvalue has exactly one dominant form factor. It is either f_j^{xx} , f_j^{yy} or f_j^{zz} . This allows to recover the fact that the correlation length associated with $C_{zz}(R)$ is halved as compared to the other two, in agreement with the exact result. This shows that such information is encoded, and can be directly extracted from MPS TM. It is worth to notice that the dominant part of TM spectrum is relatively sparse: all points in Fig. 2(b) were obtained using the information from up to 11 largest TM eigenvalues and this was enough to distinguish and extrapolate two correlation lengths differing by a factor of two, even for largest $D = 512$ used there.

In Fig. 2(c) we show the results for $g = 1.5$ illustrating that the problem with precise extrapolation is present even far away from the critical point when the correlation length is of the order of few sites only. Even in this simple case, without resorting to extrapolation, it is virtually impossible (as the smallest Schmidt values are falling below numerical precision) to recover the true correlation

length with relative error below 0.75%. On top of that the value of the relative error, say for fixed D , clearly depends on the distance from the critical point – compare with Fig. 2(a) for $g = 1.01$. This makes any fits that use correlation length obtained directly from MPS with fixed D , e.g. extracting critical exponents or the position of the critical point out of it, much less trustworthy. Proper extrapolation, as suggested in this article, allows to significantly solve this problem.

In Fig. 2(d) we show results for the Ising model in the ferromagnetic phase with $g = 0.99$. In the regime $0 < g < 1$, the correlations functions behave asymptotically as $C_{xx}(R) \sim R^{-2} \exp(-R/\xi)$, $C_{yy}(R) \sim R^{-3} \exp(-R/\xi)$, and $C_{zz}(R) \sim R^{-2} \exp(-R/\xi)$ with the inverse of the correlation length $1/\xi = \epsilon_{\text{exact}} = -2 \ln g$. All the observations made for paramagnetic phase above fully apply here as well.

Finally, in Fig. 2(e) we show the validity of the general extrapolation ansatz introduced in Eq. (15). Error, that is the distance between ϵ_1 and the exact value, is vanishing as a power law of the refinement parameter proposed in this article with the exponent close to 1. In this simple model, however, we observe that linear regression – as discussed in the text above – is sufficient and more general power law does not result in qualitatively improvement of the results in this case. Part of the reason might be that even without extrapolation relative errors are already small here – at least as compared to other, more complicated models discussed below. More importantly the exponent b is very close to 1 here.

When $1/D$ is used as a refinement parameter the error of ϵ does not follow a simple functional form as can be seen in Fig. 2(f). While it can be locally approximated by a power law it is evidently flattening making it a poor model for extrapolation. We note that the critical point is a single exception here as observed in the context of finite entanglement scaling^{21–24}.

2. Incommensurate ferromagnetic phase

In this section we focus on the incommensurate ferromagnetic part of the phase diagram of the XY model, $g^2 + \gamma^2 < 1$, where the correlation function is not vanishing monotonically but has additional oscillating term. For $g > 0$ and $0 < \gamma < 1$ the leading asymptotics of the correlation functions is $C_{xx}(R) \sim R^{-2} \exp(-R/\xi)$, $C_{yy}(R) \sim R^{-1} \exp(-R/\xi)$, and $C_{zz}(R) \sim R^{-2} \exp(-R/\xi)$, where in this case proportionally constant may contain oscillating term with frequency set by $\varphi^{XY} = 2 \arccos(g/\sqrt{1-\gamma^2})$. The correlation length is $1/\xi = \epsilon_{\text{exact}} = \ln \frac{1+\gamma}{1-\gamma}$. We present the results in Fig. 3.

In Fig. 3(a) we show full TM spectrum on a complex plane. The dominant eigenvalues form groups with well defined complex phases¹⁶, 0 and $\pm\varphi^{XY}$ respectively. They correspond to frequency of oscillations of the correlation functions. We zoom in on the φ^{XY} branch in panel

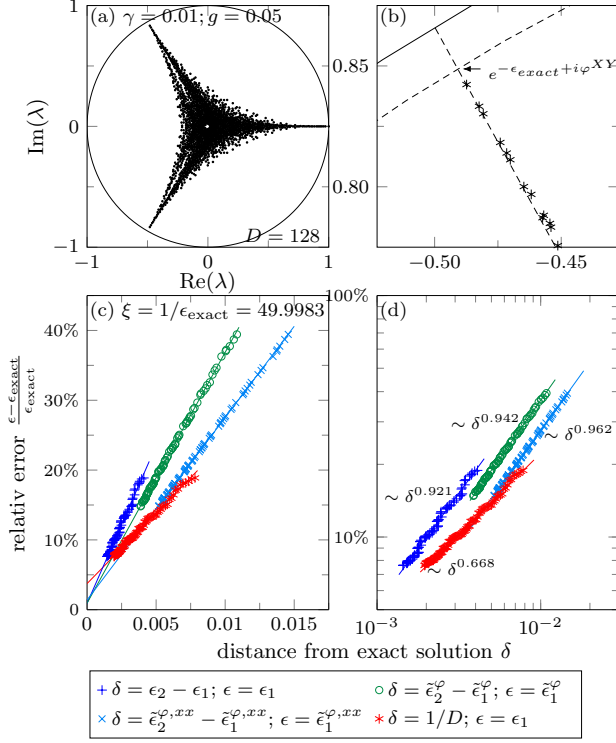


FIG. 3. (Color online) XY model in the ferromagnetic incommensurate phase, $\gamma = 0.01$ and $g = 0.5$. Panel (a) shows full TM spectrum for $D = 128$. The branch with complex angle $\simeq \varphi^{XY}$ is zoomed in panel (b), where the dashed lines show phase and modulus corresponding to the exact correlation length, respectively. We show the results of linear extrapolation in panel (c) focusing on $D = 128 \div 512$. The same data are plotted in panel (d) in a log-log scale showing the dominant power law dependence of relative error on the refinement parameter δ .

(b). It can be seen that the exact phase φ^{XY} is well reproduced in the simulation, especially for the dominant eigenvalue. In panel (c) we show results of extrapolation using linear fit. In this model, simple distance from Eq. (10) used without any additional refinement results in not-to-smooth functional dependence. Nevertheless, linear regression still reproduces exact value up to 1%. The data are significantly smoother if one focuses only on the part of TM spectrum with φ^{XY} complex phase, or additionally take into account non-zero form factors. The error resulting from linear regression is however still $\sim 1\%$. All those approaches yield much better results than linear fit as a function of $1/D$ for which the error is $\sim 4\%$. This is partially clarified in panel (d) where we present the data on a log-log plot, showing that the dependence of relative error on δ is better described by a power law with the exponent that is close to 1 in our approach. Indeed, selecting points that have the same complex phase φ^{XY} and apply non-linear fit allows to reduce the error of extrapolation further to $\sim 0.3\%$.

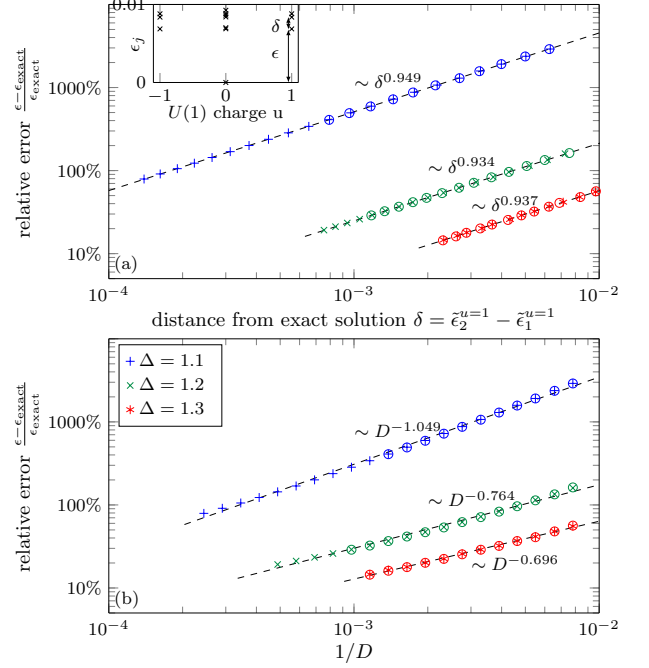


FIG. 4. (Color online) XXZ spin- $\frac{1}{2}$ model. Panel (a): Stars correspond to the error as a function of refinement parameter $\delta = \tilde{\epsilon}_2^{u=1} - \tilde{\epsilon}_1^{u=1}$, where we employ $U(1)$ symmetry and u is the symmetry charge. Inset shows splitting of the dominant part of TM spectrum into symmetry sectors for $\Delta = 1.2$ and $D = 2048$. Circles show the data obtained without employing symmetries and $\delta = \epsilon_5 - \epsilon_1$, notice near degeneracy of the dominant four TM eigenvalues in the inset. Panel (b): The same data with the modification that $\delta = 1/D$ is used as a refinement parameter. Only points for $D \geq 128$ are shown.

B. XXZ spin- $\frac{1}{2}$ model

In this section we analyze the results for spin- $\frac{1}{2}$ XXZ model

$$H = \sum_m (\sigma_m^x \sigma_{m+1}^x + \sigma_m^y \sigma_{m+1}^y + \Delta \sigma_m^z \sigma_{m+1}^z), \quad (17)$$

where we focus on massive antiferromagnetic regime $\Delta > 1$. Asymptotics of longitudinal correlation function in this regime was recently calculated in Ref. 32 as $C_{zz}(R) \sim R^{-2} e^{-R/\xi}$, see Eq. (3.36) therein for the full expression. The correlation length in the model reads $1/\xi = \epsilon_{\text{exact}} = -\log(k(q^2))$, where $q = e^{-\text{arccosh} \Delta}$ and elliptic modulus $k(q^2) = \vartheta_2^2(0, q^2)/\vartheta_3^2(0, q^2)$ with $\vartheta_n(z, q)$ being Jacobi theta function^{32–34}. To the best of our knowledge the algebraic part of the transverse correlation function $C_{xx}(R)$ is not known analytically.

The numerical results in this and in the following sections were obtained using iDMRG algorithm³⁵ with 2-site unit cell incorporating $U(1)$ symmetry^{36,37}, which in this case corresponds to conservation of $S_{\text{total}}^z = \sum_m \sigma_m^z$. All points were converged up to maximal change of Schmidt values in the last iteration below 10^{-10} . The bond di-

mensions D approximately form geometric series with a step $2^{1/4}$.

We collect the results in Fig. 4, where we focus on part of the TM spectrum corresponding to $U(1)$ charge $u = 1$ with the refinement parameter δ defined in this sector according to Eq. (14). We present the splitting of the dominant part of TM spectrum for a single D in the inset of panel (a). The panel itself shows the data in a log-log scale to highlight power law dependence of the error of ϵ on δ . For completeness, in panel (b) we show the dependence of the error on $1/D$. While it is smooth, it does not seem to follow a clear functional form again making it not very useful for precise extrapolation.

We also run simulations with VUMPS with 1-site unit cell³⁸ and without $U(1)$ symmetry where we used refinement parameter $\delta = \epsilon_5 - \epsilon_1$, as defined in Eq. (13), to take into account near-degeneracy of $\epsilon_1, \dots, \epsilon_4$ – see inset of Fig. 4(a). We present those results to show how to deal with degeneracies when they become an issue for the simplest refinement parameter in Eq. (10). Those results are represented by circles in Fig. 4. An alternative approach would be to take the suitable form factors into account. Notice that f^{zz} can be non-zero only for eigenvalues belonging to $U(1)$ charge $u = 0$. Similarly, $f^{xx} = f^{yy}$ can be non-zero only when $u = \pm 1$.

Finally, we collect results of the actual non-linear fits in Table I. The values are averaged over range of bond dimensions taken into account, where we use 8 to 13 points with largest D . Additionally, we also take into account dominant form factors. This is especially relevant for $u = 0$ sector where there is near-degeneracy of two dominant eigenvalues, which still has to be resolved (see inset of Fig. 4(a)). Apart from $\Delta = 1.1$, the exact value of the correlation length is recovered with the error well below 1%. It is $\sim 3\%$ for $\Delta = 1.1$, however the correlation length is approaching 10^4 here and we extrapolate from MPS correlations lengths underestimating the exact one by almost a factor of 2. Obtaining such results from the simulation of finite system is practically impossible showing effectiveness of the infinite uniform approach.

We finish this section with an observation that the TM spectra which we obtain from numerics in this model are real. There are both positive and negative eigenvalues for 1-site unit cell implementation (complex phases $\varphi = 0, \pi$) which corresponds to the monotonic and staggered part of the correlation function asymptotics – see Eq. (3.36) in Ref. 32. This information about phase is lost in 2-site unit cell transfer matrix, where the spectrum is effectively squared and strictly positive, which shows some advantage of using as small unit cell as possible. It is interesting to contrast this with the spectrum of the quantum transfer matrix which is complex with the complex phase changing in a continuous way, see e.g. Ref. 33 for in-depth discussion. In that case the minimal gap of the quantum transfer matrix is not dictating the actual correlation length as contributions of part of the QTM spectrum band are effectively canceling out. Apparently, MPS is capturing only the physically relevant part of the

Δ	1.1	1.2	1.3	1.4	1.5
ξ_{exact}	8482.801	347.131	85.1433	37.0497	21.0729
$\xi_{u=1}^{xx}$	8280(130)	345.9(24)	85.54(99)	37.0(10)	20.89(74)
$\xi_{u=0}^{zz}$	8200(120)	348.6(21)	85.5(12)	37.36(80)	21.12(51)
D_{max}	4096	2048	862	430	256
$\xi_{D_{\text{max}}}$	4734	291.3	74.29	32.49	18.51

TABLE I. XXZ spin- $\frac{1}{2}$ model. Comparison of the extrapolated correlation length with the analytical result. Correlation length is resolved by symmetry sector, where $u = 1$ can be associated with $C_{xx}(R)$ and $u = 0$ with $C_{zz}(R)$. Additionally, we show the largest bond dimension D used for given Δ and the corresponding MPS correlation length. For those D the exact ground state energy is reproduced up to an error of $O(10^{-14})$ for $\Delta \geq 1.2$ and $O(10^{-12})$ for $\Delta = 1.1$.

spectrum making it purely real in our case. Similar situation – though slightly more complicated – arise in the 8-vertex model which we discuss below in the context of CTM algorithm.

C. XXZ spin- $\frac{3}{2}$ model

In this section we consider spin- $\frac{3}{2}$ XXZ model

$$H = \sum_m (S_m^x S_{m+1}^x + S_m^y S_{m+1}^y + \Delta S_m^z S_{m+1}^z), \quad (18)$$

where $S_m^{x,y,z}$ are standard spin- $\frac{3}{2}$ operators acting on site m . Similarly to the spin- $\frac{1}{2}$ case discussed in the previous section, the model has a critical region for $-1 \leq \Delta \leq 1$ with a Berezinskii–Kosterlitz–Thouless (BKT) critical point at $\Delta_c = 1$ separating gapped phase for $\Delta > 1$ ^{39–42}. Again, we focus on the gapped phase, where the correlation length scales as

$$\xi(\Delta) = \xi_0 \exp(B/\sqrt{|\Delta - \Delta_c|}). \quad (19)$$

Even though the exact value of the critical point is known, the model cannot be solved exactly and the value of the correlation length is not known analytically. Additionally, it is particularly challenging to approximate the ground state due to very strong quantum fluctuations^{43,44}. As such, the model provides a good test for numerical methods. We extrapolate the correlation lengths using our method and subsequently fit the scaling form of Eq. (19) (with higher order corrections) in order to extract Δ_c and the parameter B . We collect the results in Fig. 5 and a few selected correlation lengths in Table II.

We proceed similarly as in the previous section. We define the refinement parameter by taking into account information about symmetry sector, Eq. (14), and extrapolate by fitting general power law in Eq. (15) to $8 \div 13$ points with largest bond dimension D used in simulation. Consecutive D form geometric series with a step $2^{1/4}$

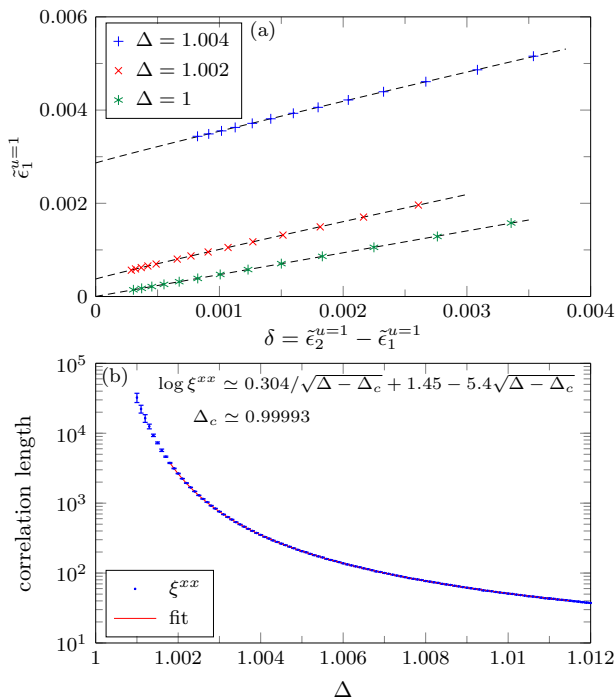


FIG. 5. (Color online) XXZ spin- $\frac{3}{2}$ model. Panel (a) shows extrapolation of the correlation length for selected values of Δ . Refinement parameter δ is calculated from sector with U(1) charge $u = 1$, Eq. (14). In panel (b) we collect correlation lengths obtained from our extrapolation procedure. Subsequently, we fit the form of $\log(\xi(\Delta))$ given in Eq. (19). This allows us to recover the exact position of the critical point, $\Delta_c = 1$, with excellent accuracy. See text for details.

approaching 10000 for the most challenging points. We show some of such fits in Fig. 5(a). This also includes the critical point at $\Delta = 1$, where we obtain the extrapolated value of inverse correlation length as $\epsilon_e \sim 10^{-6} \pm 7 \cdot 10^{-6}$, which is 2 orders of magnitude smaller than the value of ϵ_1 obtained for the largest $D = 5792$ converged here. This shows both the limits and validity of our approach, as within the estimation error we are able to recover the exact value (zero) at the critical point.

Subsequently, in Fig. 5(b), we fit $\ln \xi = a_1 + B(\Delta - \Delta_c)^{-1/2} + a_2(\Delta - \Delta_c)^{1/2}$ where we allow for sub-leading correction with non-zero a_2 to improve the quality of the results. We take into account $\xi \in [40, 4000]$, where the estimated errors of extrapolations are below 1.5%. We obtain $\Delta_c = 0.99993(4)$, which is in very good agreement with the exact value of $\Delta_c = 1$. The non-universal constant $B = 0.304(12)$, $a_1 = 1.45(20)$ and $a_2 = -5.4(12)$.

We compare those results with the ones recently reported in Ref. 43, which were obtained by fitting the scaling ansatz capturing behavior of the energy gap in the finite system. Namely $\Delta_c = 0.995 \pm 0.004$ and $B = 0.50 \pm 0.02$ ($\Delta_c = 0.989 \pm 0.01$ and $B = 0.58 \pm 0.04$) for open (periodic) boundary conditions, where the systems up to 280 (72) spins were used. We are able to access

Δ	1.002	1.004	1.006	1.008	1.01
$\xi_{u=1}^{xx}$	2654(26)	351.7(27)	137.59(94)	76.89(92)	50.90(63)
D_{\max}	9742	8192	3444	2896	512
$\xi_{D_{\max}}$	1773	290.9	115.8	65.9	41.3

TABLE II. Extrapolated correlation lengths for the XXZ spin- $\frac{3}{2}$ model. Additionally, we show maximal bond dimension D used in the simulation, as well as MPS correlation length for that D .

the range of correlation lengths which are order of magnitude larger than system sizes possible in state-of-the-art finite system simulations and also take into account sub-leading correction to the scaling – which become increasingly important at a distance from the critical point. As such, we expect our results to be more accurate, which can be seen in the precision with which we were able to localize the critical point.

D. Bose-Hubbard model

We conclude this part with the Bose-Hubbard model in one dimension,

$$H = -J \sum_m (b_{m+1}^\dagger b_m + b_m^\dagger b_{m+1}) + \frac{U}{2} \sum_m n_m (n_m - 1), \quad (20)$$

where b_m are bosonic annihilation operators acting on site m and $n_m = b_m^\dagger b_m$ is the particle number operator. Below we set the energy scale by fixing Coulomb repulsion $U = 1$ and consider system with unit filling per lattice site, $\langle n_m \rangle = 1$. The model has a quantum phase transition between gapped Mott insulator phase for $J < J_c$, and gapless superfluid phase for $J > J_c$ in the Berezinskii–Kosterlitz–Thouless universality class^{45,46}. We focus on the gapped phase and proceed identically as in the previous sections.

In the iDMRG simulations we truncate the local Fock space at 6 particles, checking that this is enough to obtain converged results. We employ U(1) symmetry, which in this case corresponds to conservation of the total particle number, $\sum_m n_m$. This model proves to be less challenging for MPS simulations than the XXZ spin- $\frac{3}{2}$ model from the previous section and all the results were obtained with bond dimension up to 5792.

We collect the results of our extrapolation procedure in Fig. 6 and in Table III. We calculate both the correlation length associated with $\langle b_0^\dagger b_R \rangle$ and $\langle n_0 n_R \rangle$ correlators. We observe that ξ^{nn} is halved as compared to $\xi^{b^\dagger b}$ within the estimated extrapolation errors, see Table III. Subsequently, we focus on $\xi^{b^\dagger b}$ which can be extrapolated with higher accuracy, and fit $\ln \xi^{b^\dagger b} = a_1 + B(J_c - J)^{-1/2} + a_2(J_c - J)^{1/2}$. We use $\xi \in [10, 5000]$ for which the estimated extrapolation errors are well below 1%. We obtain the position of the critical point as

J	0.28	0.27	0.26	0.25	0.24	0.23	0.22	0.21	0.20
$\xi_{u=1}^{b^\dagger b}$	4235(17)	772.8(32)	252.6(10)	112.6(10)	60.23(29)	36.39(16)	23.93(11)	16.69(10)	12.19(11)
$\xi_{u=0}^{nn}$	2096(24)	387.4(65)	127.5(25)	56.0(29)	30.1(17)	17.92(70)	11.99(66)	8.37(70)	6.01(55)
D_{\max}	4096	2048	1024	512	362	256	256	182	128
$\xi_{D_{\max}}$	3387	677	227	101	54.9	33.4	22.3	15.5	11.4

TABLE III. Extrapolated correlation lengths in the Bose-Hubbard model with unit filling, $\langle n \rangle = 1$. We show the correlation lengths for $\langle b_0^\dagger b_R \rangle$ and $\langle n_0 n_R \rangle$. Notice that the second one is approximately halved as compared to the first one. Additionally, we show maximal bond dimension D used in the simulation and MPS correlation length for that D .

$J_c = 0.3048(3)$ and non-universal constant $B = 1.61(4)$. Besides, $a_1 = -1.34(15)$ and $a_2 = -3.52(24)$.

For the collection of results on the critical point position obtained in multitude of different studies see Table 1 in the recent review article 46, with the current consensus of $J_c \approx 0.3$. The value obtained in Ref. 47 from studies of the energy gap in the finite DMRG simulation of up to 700 sites, where the value of B was also reported, reads $J_c = 0.3050 \pm 0.0001$ and $B = 1.59 \pm 0.03$, which are in very good agreement with our results.

To conclude, we comment that the range of estimates of the critical point position, as collected in Ref. 46, illustrates very well the complexity of such studies. It emphasizes the necessity of using methods that are unbiased and able to precisely capture extreme values of the correlation length. The former is provided by MPS based schemes, evidently seen by consistency of the results obtained using those method, see Ref. 46. The latter can be provided by working directly in the thermodynamic limit, which allows to avoid problems posed by strong finite size effects and limitations on the possible system sizes in such simulations. On the other hand, proper extrapolation scheme of the correlation length significantly lessens the systematic limitations caused by finite bond dimension always present in MPS simulations. Both al-

low us to expect excellent accuracy of the results presented here, especially as we keep in mind the quality of the data obtained for the XXZ model in the previous section.

V. CORNER TRANSFER MATRIX SIMULATIONS

In the corner transfer matrix methods infinite environment of a given site (or sites in a unit cell) in 2d tensor network is approximated by a combination of four corner C_j and four top T_j tensors of finite size, as depicted in Fig. 7(i). This allows to compute expectation values of local operators of interest as well as their correlation functions. To that end we define column-to-column transfer matrix as shown in Fig. 7(ii).

We employ general corner transfer matrix algorithm described in Ref. 48, suitable for non-symmetric problems (i.e. when corners C_j are not Hermitian) and its less expensive variant described in Ref. 49. As compared to the former one, it effectively avoids squaring small Schmidt values of the enlarged corners, which are later inverted in the algorithm. Furthermore, it reduces the leading cost of the algorithm. This allows to reach larger CTM bond dimensions, which we call D .

A. Classical 2d Ising model

2d classical Ising model can be exactly mapped on the 1d XY model^{50,51}, which we discussed in details in Sec. IV A and as such we are not going to repeat those results here.

The main point which we would like to make here is that the proposed extrapolation procedure gives essentially the same result for two algorithms: CTM method for 2d classical model and VUMPS algorithm for the corresponding XY model. CTM method was used in its symmetric^{7,8} as well as non-symmetric^{48,49} form. We conclude that the accuracy of the extrapolation method described in this article, and more generally renormalization of the exact quantum transfer matrix in CTM/MPS simulations¹⁶⁻¹⁸ is mostly independent of the particular algorithm used to obtain it.

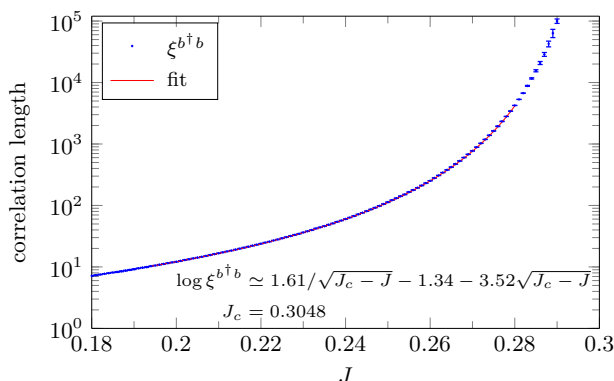


FIG. 6. (Color online) One dimensional Bose-Hubbard model with $\langle n \rangle = 1$. We show extracted values of the correlation lengths associated with $\langle b_0^\dagger b_R \rangle$ correlator. By fitting the scaling form in Eq. (19), we find the position of the critical point and non-universal constant B in this model. See text for details.

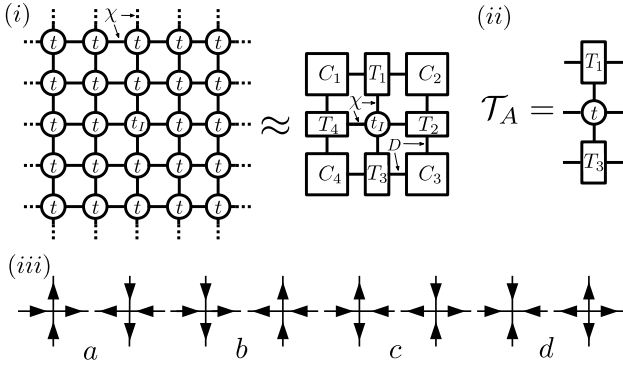


FIG. 7. (i) Visualization of the corner transfer matrix renormalization method where the environment of a single site, marked as t_I here, of infinite 2d lattice is approximated by a combination of finite size (finite D) tensors T and C . (ii) Definition of column-to-column transfer matrix used in this work. In (iii) we show allowed configurations and their Boltzmann weights in the 8-vertex model. They are combined into one tensor t in (i,ii), with $\chi = 2$ being a number of possible states of local variable living on the edges of the lattice.

B. 8-vertex model

In this section we test our approach in a numerically significantly more challenging 8-vertex model. We use the standard formulation of the model, see e.g. Refs. 33, 52, and 53, with local two-state variables living on the edges of a 2d square lattice. Each local variable is represented by an arrow pointing toward one of the two adjacent lattice vertices. Only configurations with even number of arrows pointing out of any vertex are allowed and contribution of each configuration to the partition function is calculated as a product of Boltzmann weights for each vertex, assigned as in Fig. 7(iii). The weights are parametrized as

$$\begin{aligned} a &= e^{(J+J'+J'')/T} \\ b &= e^{(-J-J'+J'')/T} \\ c &= e^{(-J+J'-J'')/T} \\ d &= e^{(J-J'-J'')/T}. \end{aligned}$$

We perform numerical tests for $J = 0.2$, $J' = J'' = 0.1$ ($a > b, c, d$). We focus on the vicinity of the continuous critical point, where the critical temperature T_c is set by the relation $a_c = b_c + c_c + d_c$. The system is in ferroelectric phase for $T < T_c$ and disordered phase for $T > T_c$. The expectation value of the vertical arrow direction serves as the order parameter in this model and the correlation length associated with this observable was calculated analytically in Ref. 33.

As this problem is in general not-symmetric (for $c \neq d$) simple CTM implementation⁷ cannot be used⁵³ and it is necessary to employ the most general CTM suitable for such problems^{48,49}. See Ref. 53 for some recent CTM studies of symmetric, but not exactly solvable modifi-

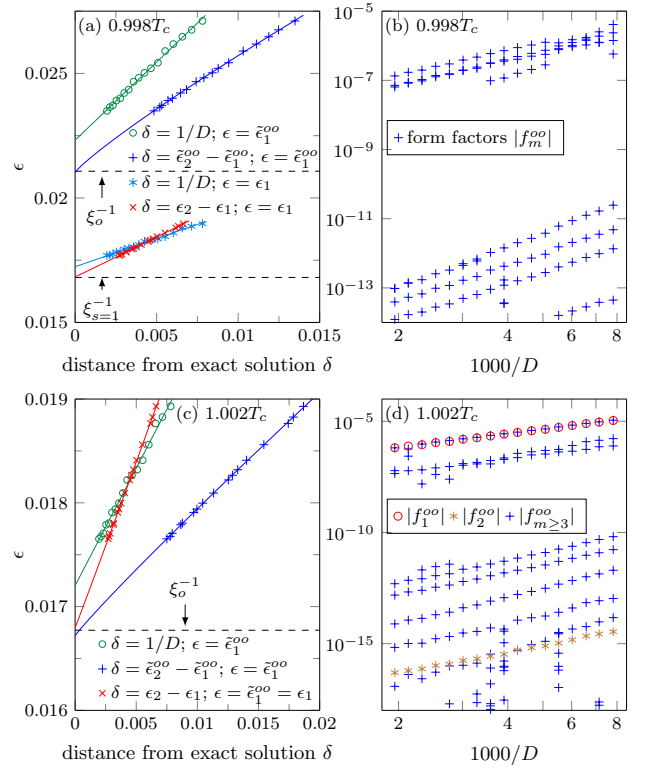


FIG. 8. (Color online) 8-vertex model with $J = 0.2$, $J' = J'' = 0.1$. Panels (a) and (c) show results of extrapolation for ferroelectric $T = 0.998T_c$ and disordered $T = 1.002T_c$ phases, respectively. Dashed lines indicate analytical results. Panels (b) and (d) show order parameter form factors for twenty largest TM eigenvalues, $D = 128 \div 512$. We use $\tilde{\zeta}_n^{oo}$ to mark the TM eigenvalues for which the order parameter form factors are non-zero in order to avoid confusion with f_n^{oo} which is the form factor corresponding to ϵ_n .

cation of this model. We show the results of simulations in Fig. 8, where we have chosen $T = 0.998T_c$ ($\xi_o = 47.4556\dots$) and $T = 1.002T_c$ ($\xi_o = 59.6230\dots$), where the correlation length is associated with the vertical arrow correlation along a row. This particular choice means that we are dealing with correlation lengths of similar order as those accessible in recent simulations of 2d quantum systems in finite temperature using variational PEPS ansatz: variational tensor network renormalization (VTNR)^{54–56}, where the method is used¹².

In the ferroelectric phase, $T = 0.998T_c$, it is necessary to focus on part of the TM spectrum that contributes to the order parameter correlation function. We define δ as in Eq. (11). The correlation length is extrapolated up to an error below 0.1% using non-linear fit, as shown in Fig. 8(a). To that end we used TM eigenvalues for which the form factors plotted in Fig. 8(b) are in the $\sim 10^{-7}$ band. The corresponding error when $\delta = 1/D$ is used is $\sim 5\%$.

It is worth to notice that TM spectrum contains another, longer scale of length obtained from the two largest

TM eigenvalues $\epsilon_{1,2}$. The order parameter form factors corresponding to those eigenvalues are zero up to the numerical precision, i.e. they are not visible in Fig. 8(b) (Note that form factors are defined as a product of two numbers of similar magnitude. This means that the values larger than 10^{-20} are considered to be non-zero). This length scale corresponds to another band of QTM eigenvalues, which however does not contribute to order parameter correlation function as the corresponding form factors vanish due to symmetries of the model⁵⁷. In order to break this symmetry we regard 8-vertex model as a special case of a more general 16-vertex model, where vertices with three-in-one-out and three-out-one-in arrows configurations are considered together with the ones already depicted in Fig. 7(iii), see e.g. Ref. 58–60. $\epsilon_{1,2}$ contributes to the correlation functions, and have non-zero form factors, for operators build from those additional vertices. The corresponding correlation length is represented by the lower dashed line in Fig. 8(a).

In the disordered phase, $T = 1.002T_c$, the situation is much simpler as the dominant eigenvalues have non-zero order parameter form factors. In Fig. 8(c) we recover the true correlation length with error $\sim 0.1\%$, both focusing on TM eigenvalues with form factors in the dominant band, $\sim 10^{-7}$ in Fig. 8(d), and by taking $\delta = \epsilon_2 - \epsilon_1$. The second one works well even though form factor for ϵ_2 (marked as stars in Fig. 8(d)) is orders of magnitude smaller than for ϵ_1 (circles).

It is worth to observe that the QTM has complex spectrum, and the above physical correlation lengths are shorter than it could have been expected from considering only the absolute value of the largest QTM eigenvalues³³. The longest scales effectively cancel out due to a combination of continuously changing complex phase of QTM eigenvalues, together with the proper symmetry of the form factors (periodicity in the space of parameters quantifying the spectrum). On the other hand the spectrum of the column-to-column TM is real and positive. It directly describes the physical length scales, which (if necessary) can be distinguish with the help of non-zero form factors corresponding to proper operators.

VI. FORM FACTORS RENORMALIZATION

In this section we focus on the behavior of the dominant form factors. We collect the data for all the models studied in this article in Fig. 9. For each D we plot the non-zero form factor and the corresponding largest TM eigenvalue. As explained below, we plot the form factors as a function of an error of an inverse correlation length, i.e. distance between $\tilde{\epsilon}_1^{oo}$ and the actual value of the correlation length inverse, ϵ_{exact} , for some correlation function $C_{oo}(R)$. In each panel, D is increased from right to left. For the models where the exact value of the correlation length is not known analytically we use the result of our extrapolation procedure.

The main observation here is that the form factors are

decreasing as a power law of an error defined above. Also, the exponent of that scaling matches the value of η in the correlation function asymptotics in Eq. (2). We base this observation on the models where η is known analytically. Indeed, for the Ising model²⁸ in the paramagnetic phase, Fig. 9(a), $\eta = 1/2, 3/2$ and 2 for $C_{xx}(R)$, $C_{yy}(R)$ and $C_{zz}(R)$ correlators, respectively. In the ferromagnetic phase, Fig. 9(b) we have $\eta = 2, 3$ and 2 for the above correlators. At the critical point, Fig. 9(c), $\eta = 1/4, 9/4$ and 2 , respectively. The above values are in very good agreement with the results of fits in Fig. 9(a-c).

For the XY model in the incommensurate phase, Fig. 9(d), the exponent $\eta = 2, 1$ and 2 , respectively. It is worth to notice that for $C_{yy}(R)$ the leading dependence, $\eta = 1$, is obtained from the sector with complex phase $\varphi = 0$, see Fig. 3(a). This is in agreement with the analytical result where the leading behavior is monotonic²⁸. The oscillating part of $C_{yy}(R)$, with frequency $\varphi = \varphi^{XY}$, appears only with larger powers of $1/R$ in the algebraic part. Indeed, this can also be seen in the scaling of the respective form factors in Fig. 9(d).

Before we discuss other models, we provide an argument why such relation is to be expected. Quite generally, starting with the quantum transfer matrix, the correlation function can be expressed as $C_{oo}(R) = \int d\vec{k} f^{oo}(\vec{k}) e^{-\epsilon(\vec{k})R}$, where $e^{-\epsilon(\vec{k})}$ are eigenvalues of QTM, parametrized by some set of continuous parameters \vec{k} and $f^{oo}(\vec{k})d\vec{k}$ are the corresponding form factors. We assume that the relevant contributions in some frequency of oscillations of the correlation function can be collected as $e^{-R/\xi} \int_0^{y_{\text{max}}} dy \hat{f}^{oo}(y) e^{-yR}$, where $y = |\epsilon(\vec{k})| - \epsilon_{\text{exact}}$, $\epsilon_{\text{exact}} = 1/\xi$. Integrated form factors are collected as $\hat{f}^{oo}(y)dy = \int^* d\vec{k} f^{oo}(\vec{k}) \delta(|\epsilon(\vec{k})| - y)$. Here the star means that we integrate over \vec{k} contributing to given frequency of correlation function oscillations. In order to obtain the asymptotics, $C_{oo}(R) \sim e^{-R/\xi} R^{-\eta}$, the integrated correlator $\hat{f}^{oo}(y)$ would have to scale as $y^{\eta-1}$ in the limit of small y .

We can view MPS TM as an approximation to the true QTM resulting from renormalisation group procedure which captures relevant degrees of freedom for the effective impurity problem along virtual (imaginary time) direction of true QTM^{16–18}. This means that the dominant eigenvalue of the TM contributing to some $C_{oo}(R)$, $\tilde{\epsilon}_1^{oo}$, should represent contributions from the range of the smallest $y \in [0, y_1]$, with $\tilde{\epsilon}_1^{oo} - \epsilon_{\text{exact}} \sim y_1$. The corresponding form factor is then obtained by averaging over the same range, $\tilde{f}_1^{oo} \simeq \int_0^{y_1} \hat{f}^{oo}(y) dy$. Collecting those results, together with the expectation that $\hat{f}^{oo}(y) \sim y^{\eta-1}$, we obtain

$$\tilde{f}_1^{oo} \sim (\tilde{\epsilon}_1^{oo} - \epsilon_{\text{exact}})^\eta. \quad (21)$$

The above argument is rather qualitative and should be understood as representing general intuition of how renormalization of the (virtual) degrees of freedom of QTM looks like in the numerical procedure leading to given MPS approximation with finite bond dimension. It

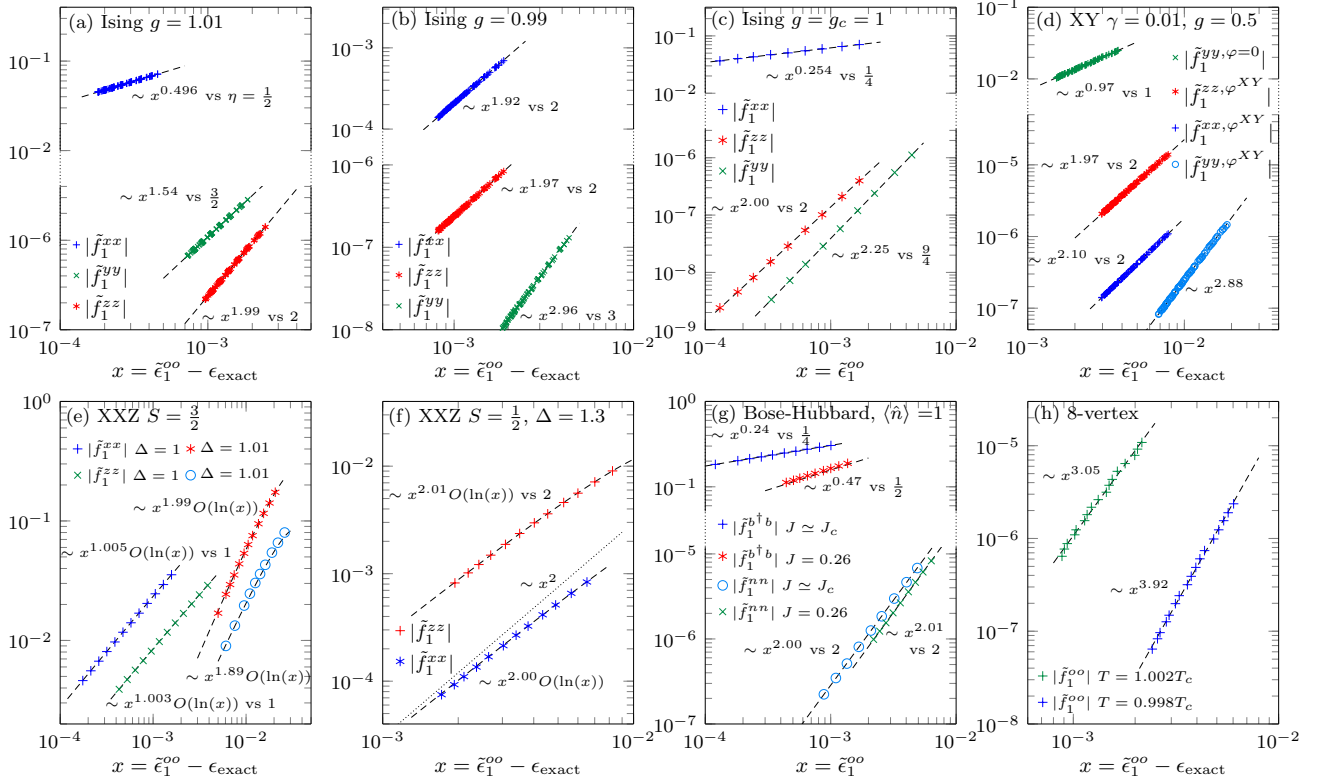


FIG. 9. (Color online) Non-zero form factors corresponding to dominant TM eigenvalues for all the models discussed in this article. We observe that they decay (as we increase the bond dimension) as a power law with the error of the inverse correlation length, $\tilde{\epsilon}_1^{oo}$, extracted directly from the transfer matrix. We observe that the exponent of the power law coincides with the corresponding exponent η of the correlation function asymptotics in Eq. (2). In each plot we show the fitted value of the exponent, as well as the value of η when we can cite the analytical result. See text for details. In each panel, the order of legend corresponds to the respective position of different lines. We remind the notation where f_n^{oo} is the form factor (for some $C_{oo}(R)$) corresponding to ϵ_n . $\tilde{\epsilon}_m^{oo}$ are the eigenvalues for which the form-factor is non-zero. Those non-zero form-factors are marked as \tilde{f}_n^{oo} .

is however hard to expect that a more formal derivation is possible, because the numerical algorithm is directly targeting variational energy as a figure of merit. At the same time it is not directly related to the full TM. Nevertheless, the results of this section give strong support to the above argument.

We can further test it in the other models considered in this article. XXZ spin chain provides an interesting example. The usual correlation function asymptotics is modified by logarithmic corrections at the isotropic critical point. It is true for spin- $\frac{1}{2}$ and spin- $\frac{3}{2}$ models. The theoretical prediction reads $C_{xx}(R) = C_{zz}(R) \sim \frac{\sqrt{\ln(bR)}}{R^\eta}$ with $\eta = 1$ ^{41,61,62}. This relation is supported by numerical studies of finite systems^{42,63}. We further corroborate this in the Appendix A using results of our iDMRG simulations. Those logarithmic corrections, which are stronger in the spin- $\frac{3}{2}$ case, should also manifest itself in the scaling of the form factors. Similarly as above, in this

case we expect the relation

$$\tilde{f}_1^{oo} \sim (\tilde{\epsilon}_1^{oo} - \epsilon_{\text{exact}})^\eta \sqrt{\ln\left(\frac{d}{\tilde{\epsilon}_1^{oo} - \epsilon_{\text{exact}}}\right)} \quad (22)$$

For XXZ spin- $\frac{3}{2}$ model at the critical point, we test it in Fig. 9(e) and obtain excellent agreement with the above prediction. The situation, however, becomes less clear in the gapped phase. For $\Delta = 1.01$ shown in the log-log Fig. 9(e), the scaling clearly deviates from the straight line, i.e. pure power law. If we assume that the vicinity of the critical point is still influencing the scaling (at least for this range of D) and allow for logarithmic corrections also in this case, then the data become consistent with $\eta \approx 2$, both for $C_{xx}(R)$ and $C_{zz}(R)$.

Such claims can be supported by analyzing the XXZ spin- $\frac{1}{2}$ model where the situation is similar, although the effects of logarithmic corrections are weaker. In the massive phase, $\Delta = 1.3$, shown in the log-log Fig. 9(f), the scaling deviates again from the clear power law. If we however assume that the logarithmic corrections are still

relevant here, we should include them in the fit using Eq. 22. This allows to recover the exponent $\eta \approx 2$ both for $C_{xx}(R)$ and $C_{zz}(R)$. In the latter case this is in very good agreement with the analytical results³², where $\eta = 2$. The dotted line $\sim x^2$ in the plot serves as a guidance for an eye.

In the Bose-Hubbard model with unit filling the situation seems to be much simpler. In Fig. 9(g) we analyse the form factors for $\langle b_0^\dagger b_R \rangle$ and $\langle n_0 n_R \rangle$ and the power law fits allow us to obtain the values of η very close to the ones predicted theoretically^{64–68}. For $J = 0.304$, very close to the critical point, we obtain $\eta = 2.00$ and $\eta = 0.24$ respectively. The exact values are 2 and $\frac{1}{4}$. In the Mott insulator phase, $J = 0.26 < J_c$, we have $\eta = 2.01$ and $\eta = 0.47$, respectively, which should be compared with the expected 2 and $\frac{1}{2}$.

Finally, in the 8-vertex model for $J = 0.2$, $J' = J'' = 0.1$ simulated here, we analyze the form factors corresponding to the order parameter. From the power law fits, see Fig. 9(h), we obtain $\eta = 3.05$ and $\eta = 3.92$ for ferroelectric ($T = 0.998T_c$) and disordered ($T = 1.002T_c$) phases respectively.

To conclude this section, few remarks are in order. We should note that the power law fits in Fig. 9 are susceptible to the value of the inverse of the true correlation length ϵ_{exact} , which is especially relevant when the exact value is not known. As a result, errors of up to a couple of percent might be expected here. Nevertheless, we can contrast the indirect approach presented here with fitting the asymptotics of the correlation function directly. As we illustrate in the Appendix A the latter can give substandard results away from the critical point within MPS simulation. As shown there, even in the simple Ising model in the ferromagnetic phase, both the values of ξ and η cannot be extracted with high accuracy from fitting Eq. (2) directly. The indirect method discussed in this section reduces the error by order of magnitude.

Finally, the data shown for all the models in this section are consistent and well described by the scaling in Eqs. (21) and (22). Additionally, they are in good agreement with the analytical values of η (when available). This allows us to get deeper understanding about the information encoded in MPS TM and its relation with the true QTM^{16–18}. It also allows us to expect good accuracy also for the models where the value of η is not otherwise known.

VII. CONCLUSION

The main message of this article is that some care has to be taken when extracting long distance properties from MPS and CTM simulations. The extrapolation procedure introduced here allows to extract the correlation length with much better accuracy than the method based on the bond dimension. In the vicinity of the critical point it can be used in parallel with the finite entanglement scaling to corroborate the results of the latter.

We use this procedure, among others, in the gapped phase of the one-dimensional Bose-Hubbard model with unit filling. This allows us to fit the scaling form of the correlation function in the vicinity of BKT critical point and extract, among others, the position of the critical point with high accuracy.

We also discuss how the algebraic part of the correlation function asymptotic is directly encoded in the scaling of the form factors. This provides new tool for calculating this quantity within MPS simulations, which, especially away from criticality, might be much better than fitting the asymptotics directly.

VIII. ACKNOWLEDGEMENT

We thank Philippe Corboz and Jacek Dziarmaga for insightful discussions. We acknowledge support by National Science Center Poland under Projects No. 2016/23/D/ST3/00384 (MMR) and 2016/23/B/ST3/00830 (PC). This research is supported in part by the U.S. Department of Energy through J. Robert Oppenheimer fellowship (LC).

Appendix A: Direct fitting of the correlation function asymptotics

In this appendix we illustrate problems related to fitting the correlation function asymptotics directly, which provides further evidence of superiority of the extrapolation scheme proposed in this article. In Fig. 10(a) we show $C_{xx}(R)$ in the ferromagnetic phase of the Ising model. We check that the results are converged in the bond dimension. We fit the asymptotic form in Eq. (2) for different ranges of the distance R to that data.

We expect three regimes of R . For relatively short distances $1 \ll R \ll \xi$ the behavior of the correlation function is still strongly influenced by the vicinity of the critical point, for which $C_{xx}(R) \sim R^{-\eta_1}$, with $\eta_1 = 1/4$ in our example. In the other extreme limit, $R \gg 1/\delta$, where $\delta = \tilde{\epsilon}_2^{xx} - \tilde{\epsilon}_1^{xx}$ is the measure of deviation from the continuous spectrum, we end up with purely exponential behavior, $e^{-R\tilde{\epsilon}_1^{xx}}$, i.e. the one in Eq. (1). This is an ultimate consequence of finite bond dimension used in the numerical simulations. Finally, let us see if one can recover the exact asymptotic, $e^{-R/\xi}R^{-\eta}$, in the intermediate regime $\xi \ll R \ll 1/\delta$. The combination of required scale separation, numerical precision and limitations imposed by finite bond dimension make this interesting limit very hard to attain in practice, especially when $\eta \neq \eta_1$ (here $\eta = 2$).

A smooth transition between such three limits can indeed be recognized in Fig. 10(a). In our example $\xi = 49.7\dots$ and $1/\delta \approx 700$ ($D = 512$), as can be read from Fig. 2(d). It is worth to observe that the largest values of locally fitted correlation length, even though they are larger than the value given by the largest TM

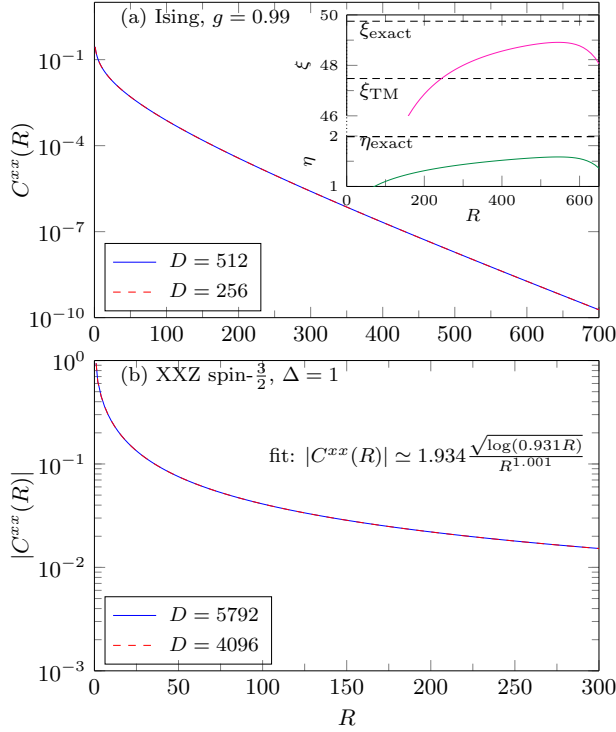


FIG. 10. (Color online) In panel (a) we show an example of direct fitting of the correlation function asymptotics from Eq. (2) for the Ising model in the ferromagnetic phase, $g = 0.99$. The results of the fit $\ln C_{xx}(r) \simeq a + r/\xi - \eta \ln(r)$ for windows of $r \in [R - 25, R + 25]$ are collected in the inset. Extracting the actual correlation function asymptotic is substandard in this case. For comparison, in panel (b) we show the correlation function for the critical antiferromagnetic Heisenberg spin- $\frac{3}{2}$ chain, which can be very well fitted with the theoretical scaling prediction. Fit done for $R \in [100, 300]$.

eigenvalue, are still almost 2% away from the exact one. Additionally, they strongly depend on the window of R 's used in the fit. As a result, extracting it in this way is not very reliable. For comparison, our extrapolation procedure gives result which is order of magnitude more accurate, see Fig. 2(d). Similarly $\eta \approx 1.5$, which is the largest local estimate in Fig. 10(a) is far from being precise. Significantly better estimate is obtained from scaling of the form factors in Fig. 9(b). We stress here that while the discussion above is quite general, the illustrative example of the Ising model is well known not to be challenging for MPS based methods. As such we could expect even more severe problems for more demanding systems.

Paradoxically, the situation at the critical point is much simpler, even though such points are generally harder to simulate with MPS. Above all, there is no physical length scale ξ in this case. As such, we can expect to recover the exact asymptotics for $1 \ll R \ll 1/\delta$, with finite D effects becoming relevant on larger distances only. This, in principle, makes direct extraction of the correla-

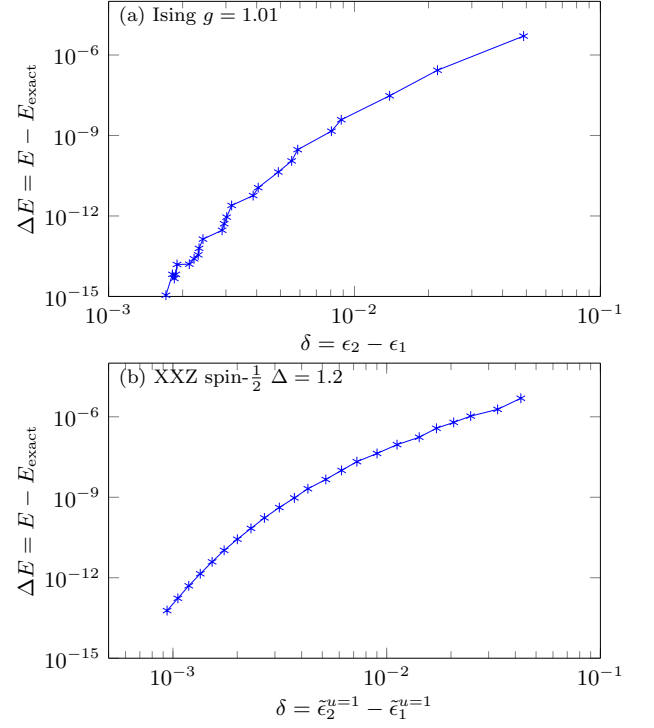


FIG. 11. (Color online) The refinement parameter δ introduced in this article is not suited for extrapolation of local quantities, such as energy. This is illustrated using the example of (a) Ising model and (b) XXZ spin- $\frac{1}{2}$ model, where we show the error of ground state energy ΔE converged for different D . In panel (a) $D = 8 \div 100$ and in (b) $D = 32 \div 1448$. This implicates that the methods which do work well for the extrapolation of the energy would not work for the correlation length.

tion function asymptotics much more straightforward in this case (there might still be problems related e.g. with spontaneous symmetry breaking resulting from finite D , or other effect of inefficient description of critical points with MPS).

As an illustrative example, in Fig. 10(b) we show $C_{xx}(R)$ for the isotropic antiferromagnetic Heisenberg spin- $\frac{3}{2}$ chain. Difference between the results for two bond dimensions shown there, as well as difference from $C_{zz}(R)$, are well below 10^{-5} . In this case the scale $1/\delta \approx 3000$, as can be read from Fig. 5(a). Correlation function asymptotics was theoretically predicted^{41,61,62} as $(-1)^R a \frac{\sqrt{\ln(bR)}}{R^\eta}$, with $\eta = 1$. From the fit to the region $R \in [100, 300]$, which is order of magnitude smaller than $1/\delta$, we obtain $a = 1.9344(81)$, $b = 0.931(19)$ and $\eta = 1.00148(41)$ with goodness of the fit $\text{SSE} = 3 \cdot 10^{-10}$, in very good agreement with the prediction. This further corroborates and improves upon the relatively old verification⁴² obtained in DMRG study of finite systems of up to 60 spins.

The above example, apart from corroborating older results, clearly shows that extracting the correlation func-

tion asymptotics from MPS simulations at the critical point is a viable method of obtaining the exponent η , unlike for the system away from criticality. Indeed, even logarithmic correction is clearly recovered in the example and has to be taken into account in the fit. Likewise, we should note that obtaining η in the critical systems from the fits to the form factors, as in Sec VI and Fig. 9(c,e,f) seems to yield comparable precision of the results. The latter method, however, proves to be superior away from the critical point.

Appendix B: Extrapolation of the local quantities

The refinement parameter δ introduced in this article proves to be well suited for extrapolation of non-local quantities such as the correlation length. The natural question is if it could be used for extrapolation of local

observables, such as energy per site or order parameter as well. To resolve this problem, in Fig. 11 we show the error of the ground state energy ΔE as a function of δ for the Ising and XXZ spin- $\frac{1}{2}$ models. The relation $\Delta E(\delta)$ is not particularly smooth and this shows that such approach is not suited for local quantities. The results presented in Fig. 11 should be compared with those in Fig. 2(a) and 4(a) for the Ising and XXZ spin- $\frac{1}{2}$ models respectively. This however allows us to argue that one should not expect a smooth relation between the error of the correlation length and the error of the ground state energy.

There are well established approaches to extrapolate the energy in MPS^{69–73}. They are based on the truncation error or the energy variance as a refinement parameter for such fits. The argument above however implies that they should not be used to extrapolate the correlation length.

-
- ¹ M. Fannes, B. Nachtergaele, and R. F. Werner, *Communications in Mathematical Physics* **144**, 443 (1992).
- ² F. Verstraete, V. Murg, and J. I. Cirac, *Advances in Physics* **57**, 143 (2008).
- ³ U. Schöllwock, *Annals of Physics* **326**, 96 (2011).
- ⁴ R. Orús, *Annals of Physics* **349**, 117 (2014).
- ⁵ S. R. White, *Phys. Rev. Lett.* **69**, 2863 (1992).
- ⁶ S. R. White, *Phys. Rev. B* **48**, 10345 (1993).
- ⁷ T. Nishino and K. Okunishi, *Journal of the Physical Society of Japan* **65**, 891 (1996).
- ⁸ T. Nishino and K. Okunishi, *Journal of the Physical Society of Japan* **66**, 3040 (1997).
- ⁹ F. Verstraete and J. I. Cirac, cond-mat/0407066 (2004).
- ¹⁰ J. Jordan, R. Orús, G. Vidal, F. Verstraete, and J. I. Cirac, *Phys. Rev. Lett.* **101**, 250602 (2008).
- ¹¹ L. Cincio, J. Dziarmaga, M.M. Rams and W.H. Zurek, *in prep.*
- ¹² P. Czarnik and P. Corboz, *in prep.*
- ¹³ F. Verstraete and J. I. Cirac, *Phys. Rev. B* **73**, 094423 (2006).
- ¹⁴ T. Kennedy, *Communications in Mathematical Physics* **137**, 599 (1991).
- ¹⁵ M. Campanino, D. Ioffe, and Y. v. Velenik, *Probability Theory and Related Fields* **125**, 305 (2003).
- ¹⁶ V. Zauner, D. Draxler, L. Vanderstraeten, M. Degroote, J. Haegeman, M. M. Rams, V. Stojevic, N. Schuch, and F. Verstraete, *New Journal of Physics* **17**, 053002 (2015).
- ¹⁷ M. M. Rams, V. Zauner, M. Bal, J. Haegeman, and F. Verstraete, *Phys. Rev. B* **92**, 235150 (2015).
- ¹⁸ M. Bal, M. M. Rams, V. Zauner, J. Haegeman, and F. Verstraete, *Phys. Rev. B* **94**, 205122 (2016).
- ¹⁹ K. G. Wilson, *Rev. Mod. Phys.* **47**, 773 (1975).
- ²⁰ T. Nishino, K. Okunishi, and M. Kikuchi, *Physics Letters A* **213**, 69 (1996).
- ²¹ L. Tagliacozzo, T. R. de Oliveira, S. Iblisdir, and J. I. Latorre, *Phys. Rev. B* **78**, 024410 (2008).
- ²² F. Pollmann, S. Mukerjee, A. M. Turner, and J. E. Moore, *Phys. Rev. Lett.* **102**, 255701 (2009).
- ²³ B. Pirvu, G. Vidal, F. Verstraete, and L. Tagliacozzo, *Phys. Rev. B* **86**, 075117 (2012).
- ²⁴ J. A. Kjäll, M. P. Zaletel, R. S. K. Mong, J. H. Bardarson, and F. Pollmann, *Phys. Rev. B* **87**, 235106 (2013).
- ²⁵ V. Stojevic, J. Haegeman, I. P. McCulloch, L. Tagliacozzo, and F. Verstraete, *Phys. Rev. B* **91**, 035120 (2015).
- ²⁶ H. Ueda, K. Okunishi, R. Krčmár, A. Gendiar, S. Yunoki, and T. Nishino, arXiv:1709.01275 (2017).
- ²⁷ In practice, we perform linear fits for fixed values of b , in the end picking the one that minimize the sum of residuals squared. Subsequently, we use the values obtained in such a way as initial parameters for non-linear fit which allows to avoid getting stuck in local minima. We use standard nonlinear fitting toolbox as implemented in Matlab.
- ²⁸ E. Barouch and B. M. McCoy, *Phys. Rev. A* **3**, 786 (2017).
- ²⁹ V. Zauner-Stauber, L. Vanderstraeten, M. Fishman, F. Verstraete, and J. Haegeman, arXiv preprint arXiv:1701.07035 (2017).
- ³⁰ J. Haegeman, J. I. Cirac, T. J. Osborne, I. Pižorn, H. Verschelde, and F. Verstraete, *Phys. Rev. Lett.* **107**, 070601 (2011).
- ³¹ J. Haegeman, C. Lubich, I. Oseledets, B. Vandereycken, and F. Verstraete, *Phys. Rev. B* **94**, 165116 (2016).
- ³² M. Dugave, F. Göhmann, K. K. Kozłowski, and J. Suzuki, *Journal of Statistical Mechanics: Theory and Experiment* **2015**, P05037 (2015).
- ³³ J. D. Johnson, S. Krinsky, and B. M. McCoy, *Phys. Rev. A* **8**, 2526 (1973).
- ³⁴ M. Dugave, F. Göhmann, K. K. Kozłowski, and J. Suzuki, *Journal of Physics A: Mathematical and Theoretical* **49**, 394001 (2016).
- ³⁵ I. P. McCulloch, arXiv:0804.2509 (2008).
- ³⁶ S. Singh, R. N. C. Pfeifer, and G. Vidal, *Phys. Rev. A* **82**, 050301 (2010).
- ³⁷ S. Singh, R. N. C. Pfeifer, and G. Vidal, *Phys. Rev. B* **83**, 115125 (2011).
- ³⁸ We used VUMPS algorithm with one-site unit cell and simulate Hamiltonian equivalent to (17) but with every second spin rotated to make the dominant interaction in the z -direction ferromagnetic. Otherwise the model spontaneously breaks translational symmetry making one-site unit cell ill suited to handle such case.

- ³⁹ H. J. Schulz, *Phys. Rev. B* **34**, 6372 (1986).
- ⁴⁰ I. Affleck and F. D. M. Haldane, *Phys. Rev. B* **36**, 5291 (1987).
- ⁴¹ I. Affleck, D. Gepner, H. J. Schulz, and T. Ziman, *Journal of Physics A: Mathematical and General* **22**, 511 (1989).
- ⁴² K. Hallberg, X. Q. G. Wang, P. Horsch, and A. Moreo, *Phys. Rev. Lett.* **76**, 4955 (1996).
- ⁴³ M. Dalmonte, J. Carrasquilla, L. Taddia, E. Ercolessi, and M. Rigol, *Phys. Rev. B* **91**, 165136 (2015).
- ⁴⁴ M. Dalmonte, E. Ercolessi, and L. Taddia, *Phys. Rev. B* **85**, 165112 (2012).
- ⁴⁵ M. P. A. Fisher, P. B. Weichman, G. Grinstein, and D. S. Fisher, *Phys. Rev. B* **40**, 546 (1989).
- ⁴⁶ K. V. Krutitsky, *Physics Reports* **607**, 1 (2016).
- ⁴⁷ J. Carrasquilla, S. R. Manmana, and M. Rigol, *Phys. Rev. A* **87**, 043606 (2013).
- ⁴⁸ P. Corboz, T. M. Rice, and M. Troyer, *Phys. Rev. Lett.* **113**, 046402 (2014).
- ⁴⁹ P. Czarnik, M. M. Rams, and J. Dziarmaga, *Phys. Rev. B* **94**, 235142 (2016).
- ⁵⁰ M. Suzuki, *Progress of Theoretical Physics* **46**, 1337 (1971).
- ⁵¹ M. Suzuki, *Progress of theoretical physics* **56**, 1454 (1976).
- ⁵² R. J. Baxter, *Exactly Solved Models in Statistical* (Dover Publications, Inc., 2007).
- ⁵³ R. Krěmár and L. Šamaj, *EPL (Europhysics Letters)* **115**, 56001 (2016).
- ⁵⁴ P. Czarnik and J. Dziarmaga, *Phys. Rev. B* **92**, 035152 (2015).
- ⁵⁵ P. Czarnik, J. Dziarmaga, and A. M. Oleś, *Phys. Rev. B* **93**, 184410 (2016).
- ⁵⁶ P. Czarnik, J. Dziarmaga, and A. M. Oleś, *Phys. Rev. B* **96**, 014420 (2017).
- ⁵⁷ See section VI.B in Ref. 33. Our example corresponds to the parameter $\mu \in (\pi/2, 2\pi/3]$ used there. The longer length scale, $\xi_{s=1}$, comes from $s = 1$ bound states.
- ⁵⁸ F. Y. Wu, *Phys. Rev. Lett.* **22**, 1174 (1969).
- ⁵⁹ M. Assis, *Journal of Physics A: Mathematical and Theoretical* **50**, 395001 (2017).
- ⁶⁰ L. F. Cugliandolo, *Journal of Statistical Physics* **167**, 499 (2017).
- ⁶¹ T. Giamarchi and H. J. Schulz, *Phys. Rev. B* **39**, 4620 (1989).
- ⁶² R. R. P. Singh, M. E. Fisher, and R. Shankar, *Phys. Rev. B* **39**, 2562 (1989).
- ⁶³ K. A. Hallberg, P. Horsch, and G. Martínez, *Phys. Rev. B* **52**, R719 (1995).
- ⁶⁴ F. D. M. Haldane, *Phys. Rev. Lett.* **47**, 1840 (1981).
- ⁶⁵ T. Giamarchi and A. J. Millis, *Phys. Rev. B* **46**, 9325 (1992).
- ⁶⁶ T. Giamarchi, *Physica B: Condensed Matter* **230-232**, 975 (1997).
- ⁶⁷ L. I. Glazman and A. I. Larkin, *Phys. Rev. Lett.* **79**, 3736 (1997).
- ⁶⁸ T. D. Kühner, S. R. White, and H. Monien, *Phys. Rev. B* **61**, 12474 (2000).
- ⁶⁹ O. Legeza and G. Fáth, *Phys. Rev. B* **53**, 14349 (1996).
- ⁷⁰ S. R. White, *Phys. Rev. B* **72**, 180403 (2005).
- ⁷¹ J. P. F. LeBlanc, A. E. Antipov, F. Becca, I. W. Bulik, G. K.-L. Chan, C.-M. Chung, Y. Deng, M. Ferrero, T. M. Henderson, C. A. Jiménez-Hoyos, E. Kozik, X.-W. Liu, A. J. Millis, N. V. Prokof'ev, M. Qin, G. E. Scuseria, H. Shi, B. V. Svistunov, L. F. Tocchio, I. S. Tupitsyn, S. R. White, S. Zhang, B.-X. Zheng, Z. Zhu, and E. Gull (Simons Collaboration on the Many-Electron Problem), *Phys. Rev. X* **5**, 041041 (2015).
- ⁷² G. Ehlers, S. R. White, and R. M. Noack, *Phys. Rev. B* **95**, 125125 (2017).
- ⁷³ C. Hubig, J. Haegeman, and U. Schöllwöck, arXiv:1711.01104 (2017).